

The Durham/UKST Galaxy Redshift Survey - VI. Power spectrum analysis of clustering

F. Hoyle, C.M. Baugh, T. Shanks, A. Ratcliffe

Department of Physics, Science Laboratories, South Road, Durham DH1 3LE.
email fiona.hoyle@durham.ac.uk

2 December 2024

ABSTRACT

We present the power spectrum analysis of clustering in the Durham/UKST Galaxy Redshift Survey. The Survey covers 1450 square degrees and consists of 2501 galaxy redshifts. The galaxies are sampled at a rate of 1 in 3 down to a magnitude limit of $b_J \lesssim 17$ from COSMOS scanned UK-Schmidt plates. Our measurement of the power spectrum is robust for wavenumbers $0.04h\text{Mpc}^{-1} \leq k \leq 0.6h\text{Mpc}^{-1}$, a decade and a half in length scale. The slope of the power spectrum for $k > 0.1h\text{Mpc}^{-1}$ is close to k^{-2} . The fluctuations that we measure can be expressed in terms of the *rms* variance in the number of galaxies in spheres of radius $8h^{-1}\text{Mpc}$ as $\sigma_8 = 1.01 \pm 0.17$. We find remarkably good agreement between the power spectrum measured for the Durham/UKST Survey and those from other optical studies, in spite of the very different sampling rates, magnitude limits and survey geometries employed, on scales up to $\lambda = 2\pi/k \sim 80h^{-1}\text{Mpc}$. On scales larger than this we find good agreement with the power measured from the Stromlo-APM Survey (Tadros & Efstathiou), but find more power than estimated from the Las Campanas Redshift Survey (Lin et al.). The Durham/UKST Survey power spectrum has a higher amplitude than the power spectrum of IRAS galaxies on large scales, implying a relative bias between optically and infra-red selected samples of $b = 1.3$. The spatial positions of the galaxies in the Durham/UKST survey are inferred from their redshifts, which distorts the pattern of clustering. We apply a simple model for this effect to the APM Galaxy Survey power spectrum – which is free from such distortions – and find a shape and amplitude that is in very good agreement with the power spectrum of the Durham/UKST Survey. This implies $\beta = \Omega^{0.6}/b = 0.60 \pm 0.35$, where Ω is the density parameter and b is the bias between fluctuations in the galaxy and mass distributions, and also suggests a one dimensional velocity dispersion of $\sigma = 320 \pm 140 \text{km s}^{-1}$. We compare the Durham/UKST power spectrum with Cold Dark Matter models of structure formation, including the effects of nonlinear growth of the density fluctuations and redshift-space distortions on the predicted power spectrum. We find that for any choice of normalisation, the standard CDM model, with density parameter $\Omega_0 = 1$ and a Hubble constant of $H_0 = 50 \text{km s}^{-1} \text{Mpc}^{-1}$, has a shape that cannot be reconciled with the Durham/UKST Survey power spectrum, unless either unacceptably high values of the one dimensional velocity dispersion are adopted or the assumption that bias is constant is invalid on scales greater than $20h^{-1}\text{Mpc}$. Over the range of wavenumbers for which we have a robust measurement of the power spectrum, we find the best agreement is obtained for a critical density CDM model in which the shape of the power spectrum is modified.

Key words: power spectra: galaxies: clusters: large scale structure

1 INTRODUCTION

Measuring the primordial power spectrum of density fluctuations in the universe is of fundamental importance in the development of a model for the formation of large scale structure. The shape and amplitude of the power spectrum

contain information about the nature of dark matter and the relative densities of dark matter and baryons. Several obstacles prevent a direct measurement of the primordial power spectrum from surveys of the local universe. The gravitational amplification of density fluctuations leads to a coupling of perturbations on different length scales. This

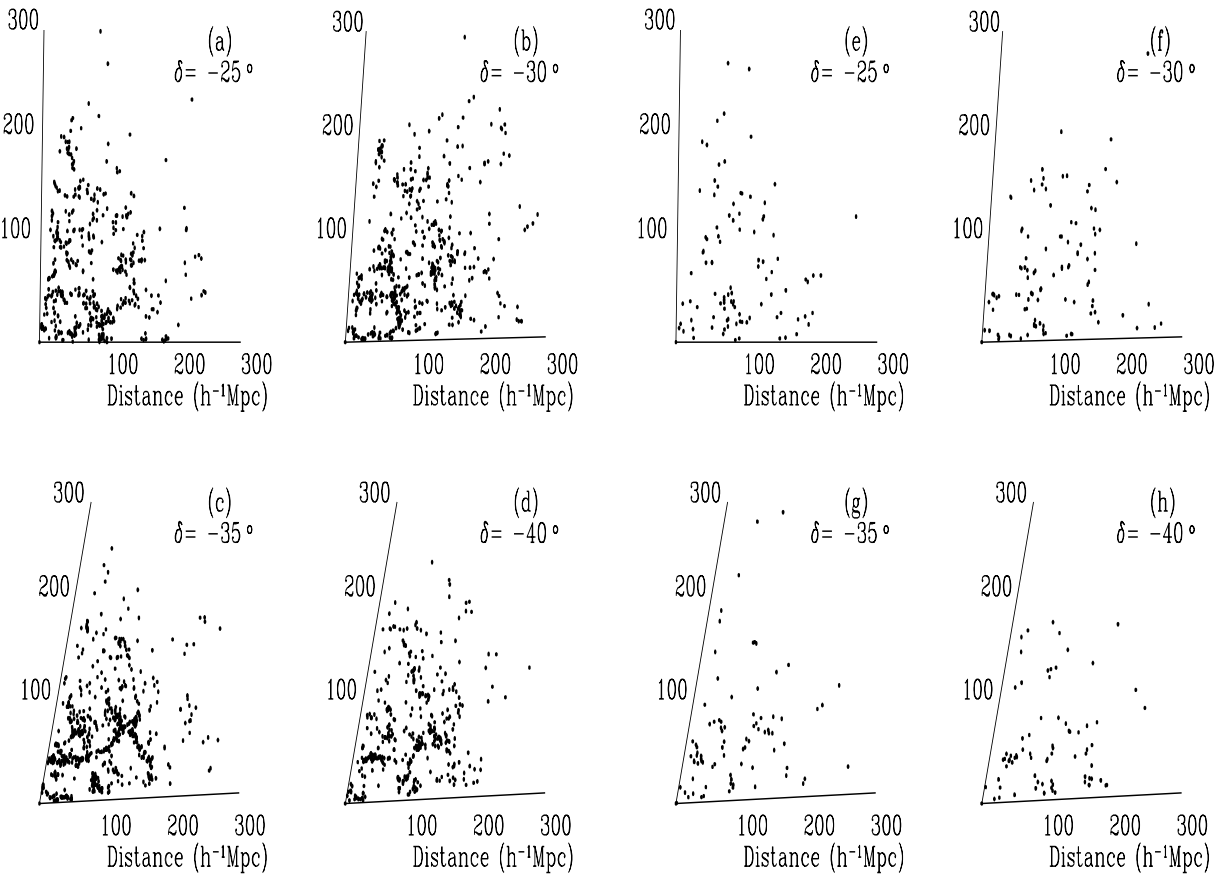


Figure 1. The four plots on the left (a-d) show the galaxies in the Durham/UKST Survey. The four plots on the right (e-h) show galaxies in the Stromlo-APM Survey which lie on the same plates. The declination slices are 5° thick and are centred on the declination shown in each panel.

results in a change in the shape of the power spectrum, except on large scales where the *rms* fluctuations are still less than unity (e.g. Peacock & Dodds 1994; Baugh & Efstathiou 1994b). Structures are mapped out by galaxies and these may be biased tracers of the underlying mass distribution (Davis et al 1985). Furthermore, the relation between fluctuations in the galaxy and mass distributions could be a function of scale and this needs to be addressed with a model for galaxy formation (e.g. Benson et al 1998). The pattern of clustering is also distorted when galaxy positions are inferred directly from their redshifts. This is due to a contribution to the observed redshift from the peculiar motion of the galaxy, that arises from inhomogeneities in the local gravitational field, in addition to the contribution from the Hubble flow (Kaiser 1987; Peacock & Dodds 1994).

Measurements of galaxy clustering have improved dramatically in the last ten years with the completion of several large galaxy surveys. The infra-red selected QDOT redshift survey (Efstathiou et al 1990; Rowan-Robinson et al 1991) and the optical, angular APM Survey (Maddox et al 1990) were the first to demonstrate that there was more power in the galaxy distribution on large scales than expected from the standard Cold Dark Matter theory of structure formation. This led to variants of the standard CDM picture being considered.

The power spectrum has become the favoured statistic for quantifying galaxy clustering. This is despite the development of improved estimators for the two-point correlation function (Hamilton 1993; Landy & Szalay 1993). Both statistics are affected by uncertainties in the mean density of galaxies, however these uncertainties affect the correlation function on all scales whereas they only affect the power spectrum on large scales. The power spectrum is also the quantity directly predicted by theory. Errors in the power spectrum are essentially uncorrelated, after taking into account the mixing of different Fourier modes due to the convolution of the power spectrum of the galaxy clustering with the power spectrum of the survey window function. Power spectra are usually estimated by a Fast Fourier transform (FFT) and are therefore relatively quick to compute. Recent theoretical work (Tegmark et al 1998) has demonstrated that power spectrum analysis can be extended to adjust for various systematic effects and biases in the data, such as obscuration by dust or the integral constraint, which we discuss in Section 4. However, in general these corrections require an assumption about the form of the underlying power spectrum and are therefore model dependent. For this reason, and because the more advanced analysis outlined by Tegmark et al (1998) has yet to be applied to any existing galaxy survey to enable a comparison, we follow the

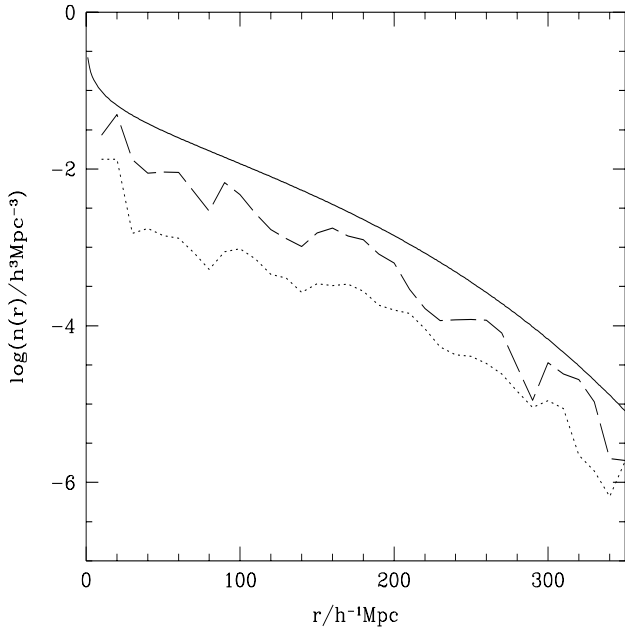


Figure 2. The solid line shows the radial number density of galaxies to a magnitude limit of $b_J \sim 17$, computed using the luminosity function of Ratcliffe et al (1998a). The dashed line shows the observed number density of Durham/UKST galaxies, which are sampled at a rate of 1 in 3 from the parent EDSGC catalogue to this magnitude limit. The dotted line shows the radial number density of galaxies in the Stromlo-APM Survey, which are sampled at a rate of 1 in 20 from the parent APM catalogue to approximately the same magnitude limit.

approach developed by Feldman, Kaiser & Peacock (1994) and Tadros & Efstathiou (1996).

We apply power spectrum analysis to the Durham/UKST galaxy redshift survey. The clustering of galaxies in this survey has been studied using the two point correlation function in earlier papers of this series (Ratcliffe et al 1996; 1998b); the magnitude of redshift space distortions was considered in Ratcliffe et al (1998c). Although the two point correlation function is the Fourier transform of the power spectrum, the same is not true of a noisy estimate of the two-point function. In addition to studying a flux limited sample, in which the galaxies are weighted such that the variance in the power spectrum estimate is minimised, we also study volume limited samples, in which all galaxies are given equal weight.

In Section 2, we describe the Durham/UKST Survey. We outline the construction of different subsamples of the Survey for power spectrum analysis in Section 3. Power spectrum estimators are tested using mock catalogues drawn from a large numerical simulation of clustering in Section 4 and we present our results in Section 5. The implications for models of large scale structure formation in the universe are discussed in Section 6 and our conclusions are given in Section 7.

2 THE DURHAM/UKST SURVEY

Full details of the construction of the Durham/UKST Survey, including the tests made of the accuracy of the measured

redshifts and of the galaxy photometry can be found in the earlier papers of this series (Ratcliffe et al 1996, 1998a,b,c,d; see also Ratcliffe 1996). Here, we restrict ourselves to a summary of the properties of the survey that are most pertinent to a power spectrum analysis of the galaxy clustering.

The Durham/UKST Survey consists of 2501 galaxy redshifts measured with the FLAIR fibre optic system (Parker & Watson 1995). The galaxies are sampled at a rate of 1 in 3 down to a magnitude limit of $b_J \sim 17$ from the parent Edinburgh-Durham Southern Galaxy Catalogue (EDSGC; Collins, Heydon-Dumbleton & MacGillivray 1988; Collins, Nichol & Lumsden 1992). The EDSGC consists of 60 contiguous UK Schmidt Telescope (UKST) plates in four declination slices, covering a solid angle of ~ 1450 square degrees.

In Figure 1, we contrast the visual appearance of the Durham/UKST Survey (four left-hand panels, a-d) with that of Stromlo-APM Survey galaxies (four right hand panels, e-h) that lie on the same UK Schmidt plates. Structures in the Durham/UKST Survey are clearly easier to pick out by eye, due to the six times higher sampling rate of this survey compared to that of the Stromlo-APM Survey. In the slices centered on $\delta = -30^\circ, -35^\circ$ and -40° , the Sculptor void is visible out to $60h^{-1}\text{Mpc}$. (Note that we define Hubble's constant as $H_0 = 100h\text{km s}^{-1}\text{Mpc}^{-1}$.) The roof of this feature is seen in the $\delta = -25^\circ$ slice.

The radial number density of galaxies in the EDSGC is shown by the solid line in Figure 2, which we have computed using the luminosity function parameters given by Ratcliffe et al (1998a). The observed radial number density of galaxies, in bins of $\Delta r = 10h^{-1}\text{Mpc}$, is shown by the dashed line for the Durham/UKST Survey and by the dotted line for the Stromlo-APM Survey. The amplitude of the Durham/UKST dashed line lies a factor of three below the solid line due to the sampling rate used. The Stromlo-APM dotted line lies approximately a factor of 20 below the solid line because the two surveys have slightly different Schechter function parameters and magnitude limits.

3 POWER SPECTRUM ANALYSIS

3.1 Sample definition

We use two types of galaxy sample in our power spectrum analysis of the Durham/UKST survey: (i) flux-limited and (ii) volume limited. In order to estimate the power spectrum of galaxy clustering in these samples, we also need to construct sets of unclustered points with the same radial and angular selection; this process is described in Section 3.2.

3.1.1 Flux-limited sample

In this case, all galaxies with measured redshifts are used. A weight is assigned to each galaxy, to take into account the radial selection function of the survey. We adopt the form of the weight proposed by Feldman, Kaiser & Peacock (1994), which minimises the variance in the estimate of the power spectrum:

$$w(r_i) = \frac{1}{1 + n(r_i)P(k)} \quad (1)$$

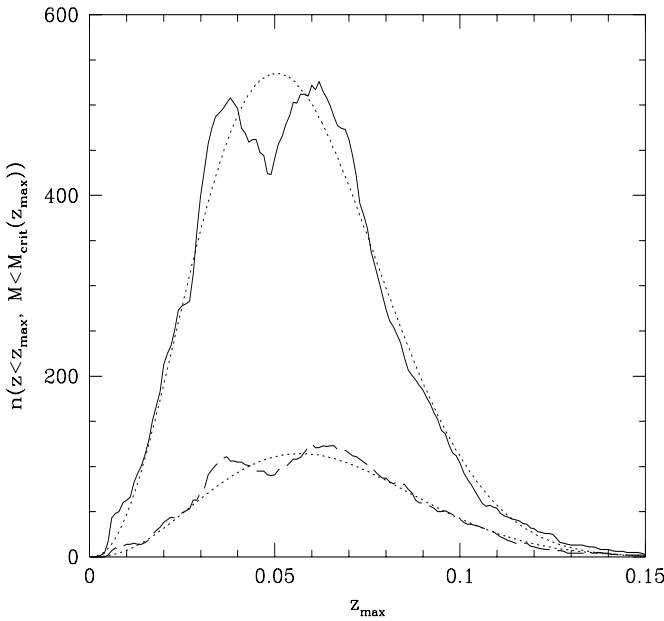


Figure 3. The number of galaxies in volume limited samples as a function of the redshift used to define the volume limit, z_{\max} . The solid line shows the number of galaxies in volume limited samples drawn from the Durham/UKST Survey. The dashed line shows the number of galaxies from the Stromlo-APM Survey that satisfy the volume limit constraints, and which lie on the same Schmidt plates. The number of galaxies in both cases peaks for a sample limited at $z_{\max} = 0.06$ – there is also a strong feature that can be seen in the two catalogues around $z_{\max} = 0.04$. The dotted lines show the expected number of galaxies obtained by integrating over the luminosity function, taking into account the different sampling rates of the two surveys.

Here $n(r_i)$ is the mean galaxy density at the position of the i^{th} galaxy. This is calculated by integrating over the luminosity function of the survey, taking into account the sampling rate. There is a slight difference in the magnitude limit of each Schmidt plate in the UKST Survey (see Figure 1 of Ratcliffe et al 1998b), so a separate radial weight function is computed for each plate. Ideally, one should use the true power spectrum in the weight given by equation 1. However, the results are fairly insensitive to the exact choice of power spectrum. Following the approach taken by Feldman et al (1994) and by Tadros & Efstathiou (1996), we adopt a range of constant values of $P(k)$ that are representative of the amplitude of the power spectrum over the wavenumbers of interest. We define the depth of the sample as the distance for which the radial weight function $w(r) = 0.5$. For our choices of constant power in equation 1, this gives depths in the range $200\text{--}320h^{-1}\text{Mpc}$. The power spectrum analysis of the flux limited catalogue therefore probes volumes in the range $1.2\text{--}4.9 \times 10^6h^{-3}\text{Mpc}^3$.

3.1.2 Volume-limited samples

The galaxies in a volume limited sample are brighter than the apparent magnitude limit of the survey when placed at any redshift up to that used to set the volume limit, $z \leq z_{\max}$. Hence, as well as requiring that a galaxy have

a redshift $z \leq z_{\max}$, the absolute magnitude of the galaxy must be brighter than:

$$M_{\text{crit}} = m_{\text{lim}} - 25 - 5 \log_{10} d_l(z_{\max}) - k(z_{\max}) \quad (2)$$

where m_{lim} is the magnitude limit of the survey and we use the k -correction given by Ratcliffe et al (1998a). Again, the different plate magnitude limits are taken into account, so for a given redshift limit z_{\max} , the critical absolute magnitude varies slightly from plate to plate. We compute the luminosity distance d_l assuming an $\Omega_0 = 1$ cosmology, although our results are insensitive to this choice due to the relatively low redshift of Durham/UKST galaxies.

In the Durham/UKST Survey, the number of galaxies in a volume limited subset peaks at a redshift of $z_{\max} = 0.06$ (Figure 3). There are 522 galaxies in this sample. There is a slightly smaller peak for a sample limited at $z_{\max} = 0.04$. This feature is particularly strong on the plate centered on $\delta = -35^\circ$. The same peaks are also seen in volume limited subsamples of the Stromlo-APM Survey when attention is restricted to those galaxies that lie on the Schmidt plates covered by the Durham/UKST Survey. The dotted lines in Fig. 3 are theoretical curves calculated by integrating over the luminosity function. The volume limited samples that we consider have maximum depths in the range $120\text{--}230h^{-1}\text{Mpc}$, and thus sample volumes of $0.2\text{--}1.8 \times 10^6h^{-3}\text{Mpc}^3$.

3.2 Survey geometry and radial selection function

The power spectrum measured directly from a galaxy survey is a convolution of the true power spectrum of galaxy clustering with the power spectrum of the survey window function. This is because the Fourier modes are orthogonal within an infinite or periodic volume, rather than the complicated geometry probed by a typical survey. The power spectrum of the survey window function is estimated by placing a large number of unclustered points, typically on the order of 100 000, within the angular area covered by the survey, using the radial selection function that is appropriate for the galaxy sample under consideration, as described above. Again, in the construction of this random catalogue, the different magnitude limits of the Schmidt plates in the Durham/UKST Survey are taken into account when the radial selection function is calculated.

Fig. 4 shows the power spectrum of the Durham/UKST Survey window function for various volume limited and flux limited samples. The top panel shows the power spectra of the window function for different volume limited samples. The width of the window function power spectrum decreases as the volume limit adopted increases. Figure 4(b) shows the window function power spectra of flux limited samples. As the value of the power used in equation 1 is increased, the flux limited sample has a larger effective depth and so the width of the window function is reduced. There is a relatively small change in the width of the survey window function when different samples of the data are considered. Defining the effective width of the window function as the wavenumber at which the power spectrum of the window function falls to half its maximum value, we obtain $\delta k \sim 0.015h\text{Mpc}^{-1}$. At wavenumber separations smaller than this, our estimates of the power will be strongly correlated. For both flux limited and volume limited samples,

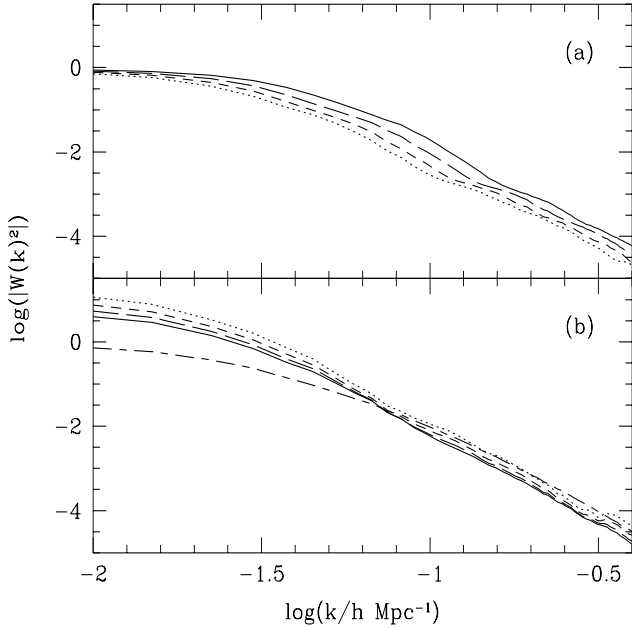


Figure 4. The two panels show the power spectrum of the window function for different samples extracted from the Durham/UKST survey. In (a), the samples are volume limited with a maximum redshift of $z_{\text{max}}=0.05, 0.06, 0.07, 0.08$ reading from top to bottom. In (b), we plot the power spectrum of the survey window function for flux limited samples. The weights applied are $P=32000, 16000, 8000, 4000$ and $0 h^{-3} \text{Mpc}^3$ reading from top to bottom at $\log k = -1.5$. For wavenumbers $k \geq 0.06 h \text{Mpc}^{-1}$, the window function power spectrum is a steep power law, $\propto k^{-4}$.

the window function power spectrum is a very steep power law at wavenumbers $k \geq 0.06 h \text{Mpc}^{-1}$, varying as k^{-4} .

3.3 Power spectrum estimation

The Fourier transform of the observed galaxy density field is given by

$$\hat{w}_o(\mathbf{k}) = \sum_i w_{\text{gal}}(\mathbf{x}_i) e^{i\mathbf{k} \cdot \mathbf{x}_i}, \quad (3)$$

where the weight function $w_{\text{gal}}(\mathbf{x}_i)$ depends upon the type of galaxy sample under consideration (note that our notation differs slightly to that used by Tadros & Efstathiou 1996). For the case of a volume limited sample, $w_{\text{gal}}(\mathbf{x}_i) = 1$ for a galaxy which satisfies the criteria given in Section 3.1.2 and $w_{\text{gal}}(\mathbf{x}_i) = 0$ otherwise. For a flux limited sample, $w_{\text{gal}}(\mathbf{x}_i)$ is given by equation 1.

The Fourier transform of the survey window function is defined by:

$$\hat{W}_e(\mathbf{k}) = \sum_i w_{\text{ran}}(\mathbf{x}_i) e^{i\mathbf{k} \cdot \mathbf{x}_i}, \quad (4)$$

where w_{ran} is the weight assigned to one of the unclustered points used to trace out the survey volume.

The power spectra of the survey window function, shown in Figure 4, are much steeper than the expected galaxy power spectrum, falling off as $\propto k^{-4}$ for wavenumbers $k > 0.06 h \text{Mpc}^{-1}$. Therefore the main effect of the convolution

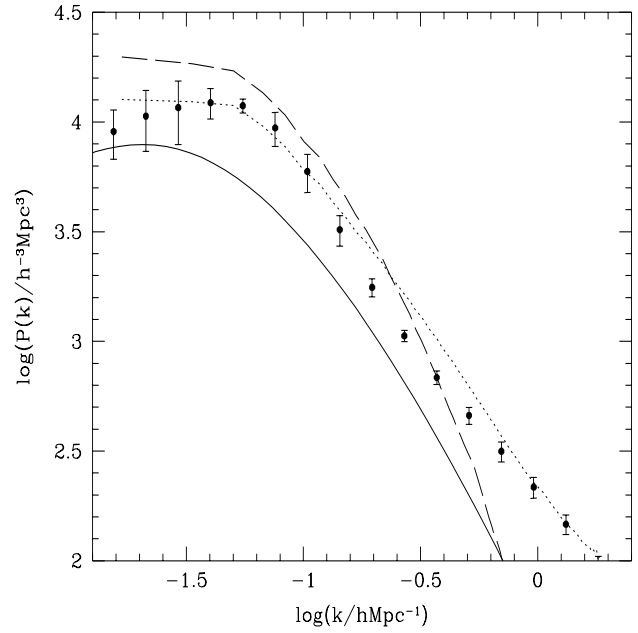


Figure 5. The solid line shows the linear power spectrum of the mass in the Hubble Volume simulation. The dotted line shows the power spectrum of a subset of the particles in the simulation, selected according to the biasing prescription outlined in Section 3.4, measured in a cubical volume of side $375 h^{-1} \text{Mpc}$. The dashed line shows the power spectrum of these biased particles when the density is binned using redshift space coordinates. The points show the power spectrum of APM Survey galaxies, measured in real space.

tion with the survey window function is to alter the shape of the power spectrum only at wavenumbers $k < 0.06 h \text{Mpc}^{-1}$.

Following the derivation outlined in Tadros & Efstathiou, we define a quantity with a mean value of zero:

$$\Delta(\mathbf{k}) = \hat{w}_o(\mathbf{k}) - \alpha \hat{W}_e(\mathbf{k}). \quad (5)$$

The power spectrum of galaxy clustering is then estimated using:

$$P_e(k) = \frac{V \left(\sum_{i=1}^{N_r} w_{\text{ran}}^2(\mathbf{x}_i) \right)^2}{\sum_{k'} |W(k')|^2} \times \left(\frac{|\Delta(k)|^2}{\left(\sum_{i=1}^{N_g} w_{\text{gal}}^2(\mathbf{x}_i) \right)^2} - \frac{1}{\sum_{i=1}^{N_g} w_{\text{gal}}^2(\mathbf{x}_i)} - \frac{1}{\sum_{i=1}^{N_r} w_{\text{ran}}^2(\mathbf{x}_i)} \right) \quad (6)$$

The power spectra are computed by embedding the Durham/UKST volume into a larger cubical volume. The density field is typically binned onto a 256^3 mesh using nearest gridpoint assignment (we discuss the effects of aliasing and box size in Section 4). The Fourier transform is performed with a FFT.

3.4 Error analysis

We estimate the errors on the recovered power spectrum by constructing mock catalogues that have the same radial and angular selection as the Durham/UKST Survey and which have approximately the same clustering amplitude.

We extract mock Durham/UKST catalogues from the

largest cosmological simulation performed to date, the *Hubble Volume*.^{*} The simulation uses 10^9 particles in a volume of $8 \times 10^9 h^{-3} \text{Mpc}^3$ and thus contains roughly 10000 independent Durham/UKST Surveys volume limited to $z_{\text{max}} = 0.06$. This allows a wide range of clustering environments to be sampled, giving a good assessment of the size of the cosmic variance for the Durham/UKST Survey.

The power spectrum of the Hubble Volume simulation is a variant of the standard Cold Dark Matter (CDM) model known as τ CDM. The shape of the power spectrum can be described by the parameter Γ , which is set to the value $\Gamma = 0.21$ for τ CDM, compared with the standard CDM case where $\Gamma = \Omega h = 0.5$ (The power spectrum used in the Hubble Volume simulation follows the definition of Γ used by Efstathiou, Bond & White 1992). This change to the power spectrum could be achieved by postulating a massive neutrino whose decay produces an additional contribution to the radiation density of the universe, delaying the epoch of matter radiation equality (White, Gelmini & Silk 1995).

The *rms* density fluctuations in the simulation are set to be roughly consistent with the local abundance of hot X-ray clusters (White, Efstathiou & Frenk 1993; Eke, Cole & Frenk 1996). The variance in the mass contained within spheres of radius $8h^{-1}\text{Mpc}$ is $\sigma_8 = 0.6$. This is smaller than found for the galaxies in the APM Galaxy Survey, where $\sigma_8^{\text{gal}} = 0.84 - 0.96$ (Baugh & Efstathiou 1993; Maddox, Efstathiou & Sutherland 1996). In order to make an accurate assessment of the errors in our recovered power spectrum we need to make mock catalogues in which the clustering matches as closely as possible that in the Durham/UKST Survey. To extract such catalogues from the Hubble Volume, we apply a simple biasing prescription to the density field. We first bin the density field onto a cubical grid of cell size $5h^{-1}\text{Mpc}$, using a nearest gridpoint assignment scheme. We then associate a probability with each grid cell, which depends on the ratio of the cell density to the mean density, for selecting a mass particle from that cell to be a biased or ‘galaxy’ particle. The form of the probability that we adopt is the same as model 1 of Cole, Hatton, Weinberg & Frenk (1998) (although these authors apply a Gaussian filter to smooth the density field - we have chosen the size of our cubical grid cell to roughly match the effective volume of the Gaussian filter):

$$P(\nu) = \begin{cases} \exp(\alpha\nu + \beta\nu^{3/2}) & \text{if } \nu \geq 0 \\ \exp(\alpha\nu) & \text{otherwise} \end{cases} \quad (7)$$

where ν is the number of standard deviations away from the mean for the density in the cell and we set $\alpha = 1.26$ and $\beta = -0.45$. The power spectrum of the biased set of particles is shown by the dotted line in Figure 5, which agrees well with the amplitude of the power spectrum of APM galaxies (Baugh & Efstathiou 1993; Gaztañaga & Baugh 1998). The

^{*} The Hubble Volume simulation was performed by the “Virgo consortium for cosmological simulations”. This is an international collaboration involving universities in the UK, Germany and Canada. The members of this consortium are: J. Colberg, H. Couchman, G. Efstathiou, C. Frenk (PI), A. Jenkins, A. Nelson, J. Peacock, F. Pearce, P. Thomas, and S. White. G. Evrard is an associate member. The Hubble Volume simulation was carried out on the Cray-T3E at the Max-Planck Rechen Zentrum in Garching.

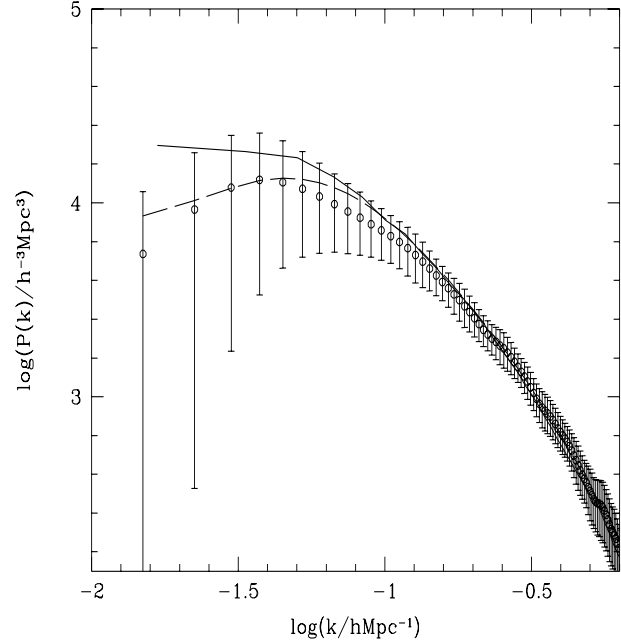


Figure 6. The solid line shows the power spectrum for samples of particles that are biased tracers of the mass distribution, averaged over 40 cubical volumes of side $375h^{-1}\text{Mpc}$ drawn from the Hubble Volume simulation. The redshift space positions of the particles are used to assign each particle to a cubical density grid. The open circles show the power spectrum averaged over 40 mock Durham/UKST catalogues made from the biased particles, to a volume limit of $z_{\text{max}} = 0.06$. We have used the actual number of galaxies extracted from the simulation in the estimator for the power spectrum (equation 6). The errorbars on these points are the 1σ errors for a single power spectrum extracted from the Durham/UKST survey. The dashed line shows the convolution of the mean power spectrum measured from the large cubical volumes (solid line) with the window function of the Survey, as shown in Figure 4.

dashed line in Figure 5 shows the power spectrum of the biased points when redshift space distortions are also included in the positions of the galaxies. As expected the power is increased on large scales and damped on small scales.

The errors on the Durham/UKST Survey power spectrum are taken to be the same size as the fractional errors on the mock catalogue power spectra. This is a valid assumption when either the contribution of shot noise to the power spectrum is negligible or, as in our case by design, the mock catalogue power spectrum and the Durham/UKST power spectrum have similar shapes and amplitudes. The errors obtained from the mock catalogues converge when averaged over 40 mock observers and are in reasonable agreement with the size of the errors obtained using the expression given in Equation 2.46 of Feldman et al (1994).

4 TESTS OF THE POWER SPECTRUM ESTIMATION

In this Section, we make systematic tests of the power spectrum estimator (equation 6) in order to assess the range of wavenumbers over which we can make a robust measurement of the true power spectrum of galaxy clustering.

On large scales there are two main effects that can cause the recovered power spectrum to differ from the true power spectrum. First, Figure 4 shows that the assumption that the power spectrum of the survey window function is sharply peaked does not hold for wavenumbers $k \leq 0.04h\text{Mpc}^{-1}$. On these scales, the recovered power spectrum has a different shape to the underlying power spectrum; the convolution of the power spectrum of the survey window function with the true galaxy power spectrum alters both the shape and amplitude of the estimated power spectrum at these wavenumbers. Second, the number of galaxies used in equation 6 is estimated from the sample itself. If fluctuations in galaxy density exist on the scale of the survey, this number can be sensitive to the environment sampled by the mock catalogue, and hence can be different from the true mean galaxy density, which is obtained by considering a much larger volume. This leads to an underestimate of the power on large scales (Peacock & Nicholson 1991; Tadros & Efstathiou 1996) which is sometimes called the integral constraint. In addition, there will be a contribution to this effect from Poisson sampling noise, even in the absence of clustering on the scale of the survey.

The power spectrum of a set of biased tracers of the mass distribution in the Hubble Volume simulation is shown in Figure 6. The redshift space coordinates of the particles have been used to assign the particles to a cubical density grid. The mean power spectrum is obtained by averaging over 40 cubical volumes of side $375h^{-1}\text{Mpc}$. The power spectrum averaged over 40 mock UKST catalogues made from the biased particles, using redshift space coordinates is shown by the open circles. The errorbars show the 1σ variance over the 40 mock catalogues. We have used the number of galaxies in the extracted mock catalogue to compute the number density of galaxies for use in the estimator (equation 6). There are still density fluctuations over volumes of the size of the Durham/UKST Survey, which leads to a variance in the number of galaxies between different mock observers and causes a bias in the power spectrum estimate at large scales. The dashed line shows the convolution of the mean power spectrum averaged over large cubical volumes (shown by the solid line) with the window function of the Durham/UKST Survey. This shows that the dominant effect on the shape of the power spectrum on large scales, is the window function convolution rather than the integral constraint for the Durham/UKST Survey. The convolution with the window function power spectrum introduces curvature into the recovered power spectrum at larger wavenumbers, $k \sim 0.05h\text{Mpc}^{-1}$, than the real turnover in the τCDM power spectrum, which occurs at $k \sim 0.02h\text{Mpc}^{-1}$.

The Fourier transform of the galaxy density field is computed by binning the galaxy density field onto a finite grid and then performing a Fast Fourier Transform (FFT). This can lead to spurious features in the power spectrum or aliasing of power on scales around the Nyquist frequency of the FFT grid. The magnitude of this effect is also sensitive to the scheme used to assign galaxies to the density grid. Figure 7 shows a series of tests designed to show the scales at which aliasing can distort the shape of the recovered power spectrum. In Figure 7(a), we vary the dimension of the FFT grid within a fixed box size of $1600h^{-1}\text{Mpc}$, whilst in Figure 7(b), we vary the size of the box in which the mock catalogue is embedded for the FFT, and keep the dimension of

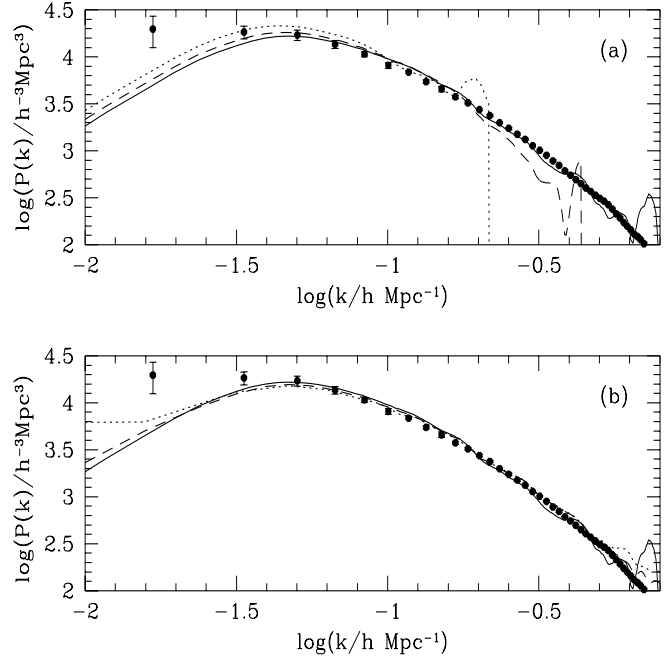


Figure 7. The solid points in (a) and (b) show the redshift space power spectrum of a set of particles extracted from the Hubble Volume simulation that are biased tracers of the mass distribution. This power spectrum has been estimated in large, cubical volumes and the errorbars show the variance over 40 such volumes. In (a), we show the effects of changing the size of the FFT grid when the mock catalogue is embedded in a fixed size box of side $1600h^{-1}\text{Mpc}$. The solid line shows the result when the density grid has 256 cells per side, the dashed line has 128 cells per side and the dotted line has 64 cells per side. In (b) we vary the size of the transform box at a fixed FFT grid size of 256 cells per side. The solid line shows the results for a transform box of $1600h^{-1}\text{Mpc}$, the dashed line for $800h^{-1}\text{Mpc}$ and the dotted line for $400h^{-1}\text{Mpc}$.

the FFT grid fixed at 256^3 . Figure 7(b) shows that using a 256^3 FFT grid and a box size of $800h^{-1}\text{Mpc}$, gives accurate results down to $k \sim 0.6h\text{Mpc}^{-1}$ or $10h^{-1}\text{Mpc}$.

As we cannot infer the true mean density of galaxies from the single observed realisation of the galaxy distribution that we have, or equivalently, we do not know the shape of the true power spectrum on these scales, we do not attempt to correct the power spectrum at large scales for either the ‘integral constraint’ bias or for the convolution with the power spectrum of the survey window function. Instead, our tests in this section demonstrate that our estimates of the power spectrum for the Durham/UKST Survey should be a robust measurement of the true galaxy power spectrum over the wavenumber range $0.04h\text{Mpc}^{-1} \leq k \leq 0.63h\text{Mpc}^{-1}$; this corresponds to a wavelength range, defined as $\lambda = 2\pi/k$, of $160h^{-1}\text{Mpc}$ to $10h^{-1}\text{Mpc}$; the latter is roughly the mean separation of galaxies in a volume limited sample.

5 RESULTS

In this Section, we analyse volume limited and flux limited samples drawn from the Durham/UKST Galaxy Redshift Survey. In all cases, the power spectra are computed by em-

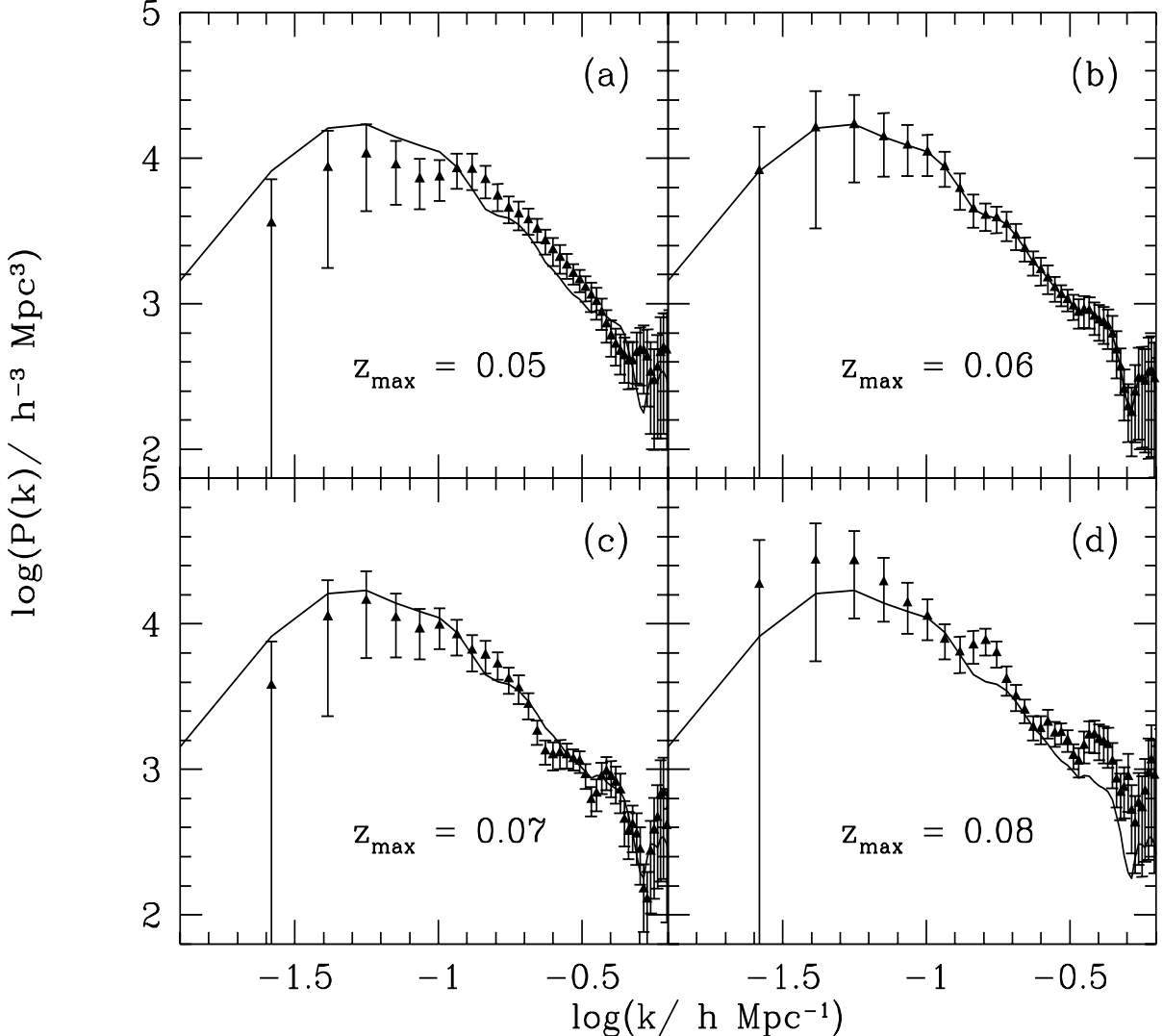


Figure 8. The power spectrum of the Durham/UKST Survey for different volume limited samples. The error bars are the 1σ variance obtained from the fractional errors on the power found in mock catalogues with the same angular and radial selection and approximately the same clustering. The power spectra are estimated using a box of side $840h^{-1}\text{Mpc}$ and a 256^3 FFT grid. The solid line is the mean power for a volume limit defined by $z_{\text{max}} = 0.06$, the sample that contains the most galaxies, and is reproduced in each panel.

bedding the survey in a box of side $840h^{-1}\text{Mpc}$ and binning the density of galaxies on a grid of 256 cells on a side. We have rebinned the estimated power spectrum in bins of width $\delta k = 0.015h\text{Mpc}^{-1}$, roughly the width at half maximum of the survey window function, in order to reduce the correlations between the estimated power at adjacent wavenumbers. A table of selected results is given in the Appendix.

The power spectra of different volume limited samples of the Durham/UKST Survey are shown in Figure 8. The errorbars are computed using the fractional variance in the power averaged over mock catalogues extracted from the Hubble Volume simulation. These mock catalogues were made for each volume limit. As discussed in Section 3.4, these catalogues satisfy the same selection criteria and have approximately the same clustering as the Durham/UKST Survey galaxies. Varying the maximum redshift used to define the volume limited catalogue has two effects on the prop-

erties of the extracted sample. Increasing z_{max} increases the depth of the sample, thereby allowing fluctuations on larger scales to be probed. At the same time however, the corresponding absolute magnitude limit imposed on the galaxies selected gets brighter. This means that the population of galaxies used to map out the clustering varies and it is possible that intrinsically brighter galaxies could be more strongly clustered than fainter galaxies (Park et al 1994; Loveday et al 1995). There is a shift in the amplitude of the power spectrum as larger values of z_{max} are considered. However, the power spectra of the different samples are all consistent within the 1σ errors.

The clustering in the flux limited Durham/UKST Survey is shown in Figure 9. Again, the errorbars show the 1σ errors obtained from the fractional variance over the power estimated from mock catalogues made with the same selection criteria. The different panels are for weight functions

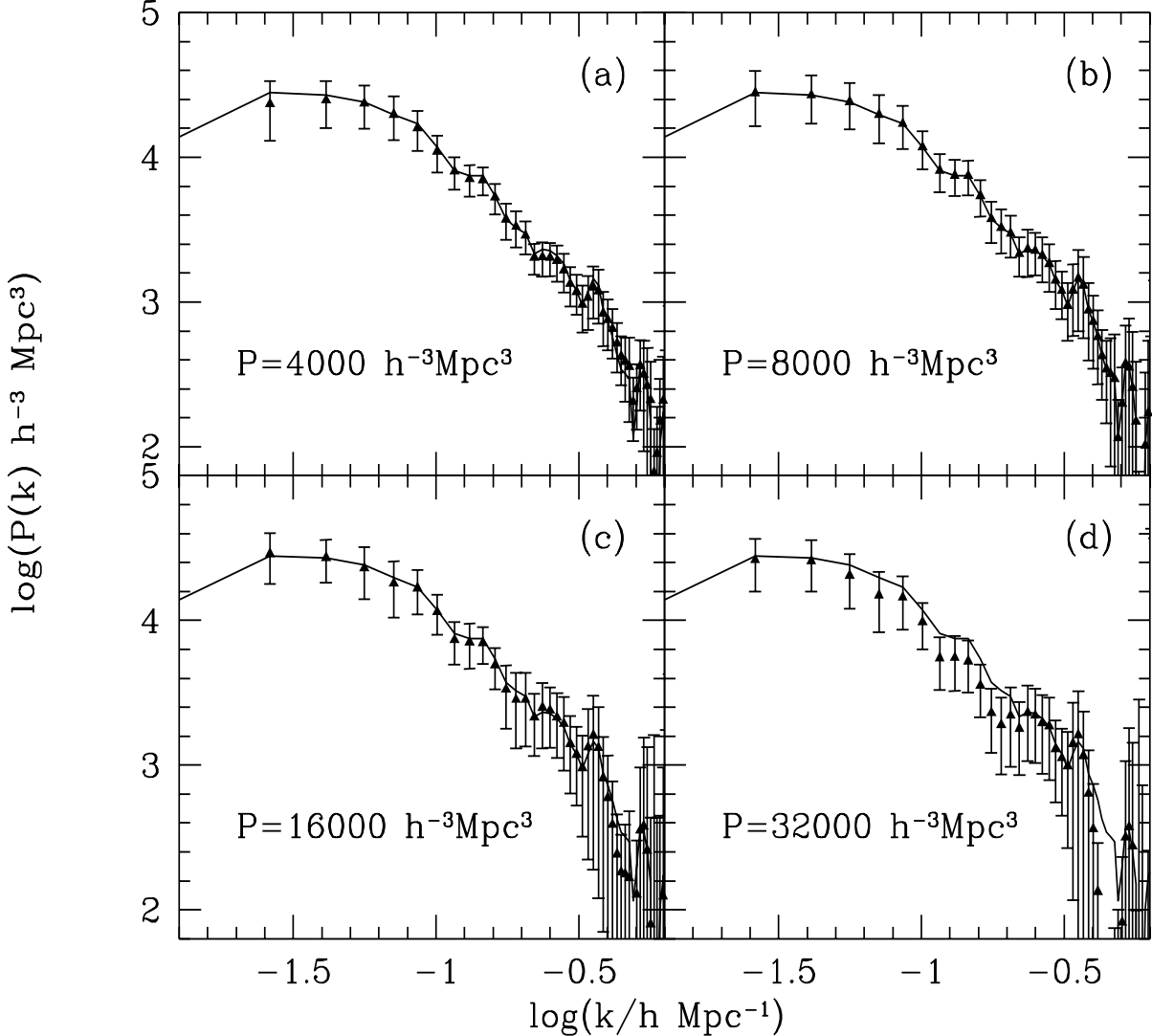


Figure 9. The power spectrum of the flux limited Durham/UKST Survey, for different constant values of $P(k)$ used in the weight function given in equation 1. The values of $P(k)$ used are $4000, 8000, 16000$ and $32000 h^{-3} \text{Mpc}^3$ as marked in the panels. The errorbars show the 1σ variance obtained from mock catalogues with the same selection and similar clustering. The solid line is the power spectrum for a weight with $P(k) = 8000 h^{-3} \text{Mpc}^3$ and is reproduced in all the panels. The power spectra are computed in a box of side $840 h^{-1} \text{Mpc}$ using a 256^3 density grid.

(equation 1) using a range of constant values for the power spectrum, as indicated in the legend on each panel. Increasing the value of the power used in the weight function, causes the weight function to rise at progressively larger distances (see Figure 3 of Feldman et al 1994). This means that the effective volume probed increases and thus the sensitivity to longer wavelength fluctuations increases.

If there are no systematic problems with the survey, changing the value of the power used in the weight function defined by equation 1 should have little effect upon the amplitude of the recovered power spectrum (see the power spectrum analysis of the combined 1.2Jy and QDOT surveys by Tadros & Efstathiou 1995). However, the size of the errors on a particular scale will change, depending upon whether or not the choice of weight function used really is

the minimum variance estimator for the amplitude of power at these scales.

The line that is reproduced in each panel of Figure 9 shows the power estimated for a weight function with $P(k) = 8000 h^{-3} \text{Mpc}^3$. This reference line shows that there is a negligible change in the mean power when this weight is varied by a factor of eight over the range $P(k) = 4000-32000 h^{-3} \text{Mpc}^3$. The flux limited power spectrum with a weight $P(k) = 4000 h^{-3} \text{Mpc}^3$ has the smallest errorbars over the range of wavenumbers plotted, though the errors are not significantly larger for the other estimates of the power spectrum. The errors on the power spectrum measured from the volume limited sample with $z_{\text{max}} = 0.06$ are larger than the errors on the power obtained from the flux limited sample for wavenumbers $k < 0.1 h \text{Mpc}^{-1}$; however, for wavenumbers

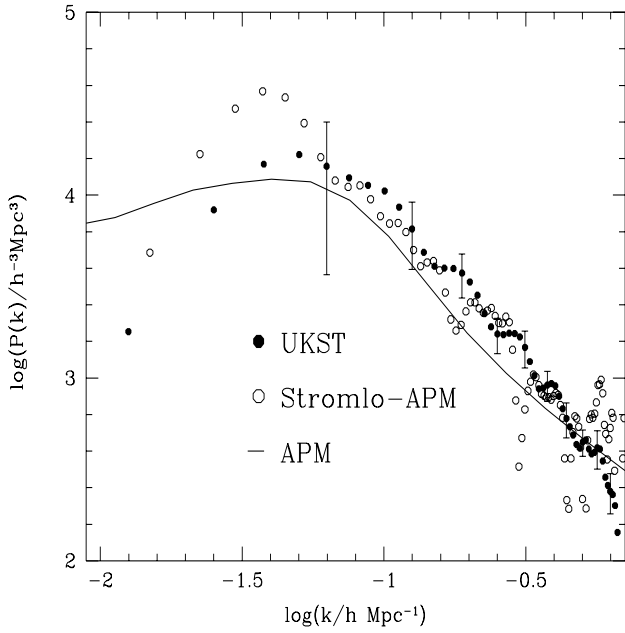


Figure 10. The volume limited power spectrum of the Durham/UKST Survey (solid points) compared with the power spectrum of the Stromlo-APM Survey (Tadros & Efstathiou 1996); in both cases, the volume limit is defined by $z_{\max} = 0.06$. The solid line shows the real-space APM galaxy power spectrum from Baugh & Efstathiou (1993).

$k > 0.1h\text{Mpc}^{-1}$ the power spectrum of the volume limited sample has smaller errors.

The comparison between the power spectra of the flux limited and volume limited samples is difficult to interpret. Neither the volume nor the way in which the volume is weighted can be simply related between the two methods for constructing galaxy samples. Furthermore, volume limited samples select intrinsically brighter galaxies as the volume is increased and it is possible that these galaxies could have different clustering properties compared with fainter galaxies. Nevertheless, the agreement between the power spectra measured from the flux and volume limited samples is very good; if we compare the power spectrum from the volume limited sample with $z_{\max} = 0.06$, which contains the most galaxies, and the power spectrum with the smallest errors from the flux limited survey (i.e. with a value of $P(k) = 4000h^{-3}\text{Mpc}^3$ used in the weight function), then the level of agreement is within the 1σ errors. This is a further argument against a significant dependence of clustering strength upon intrinsic luminosity within the survey.

6 COMPARISON WITH OTHER MEASUREMENTS OF THE POWER SPECTRUM

We compare our results with measurements of the power spectrum made from other surveys in Figures 10, 11 and 12. In Fig. 10, we compare the power spectrum from a sample of the Durham/UKST Survey, defined by a volume limit of $z_{\max} = 0.06$ (filled circles) with the power spectrum of a sample drawn from the Stromlo-APM Survey

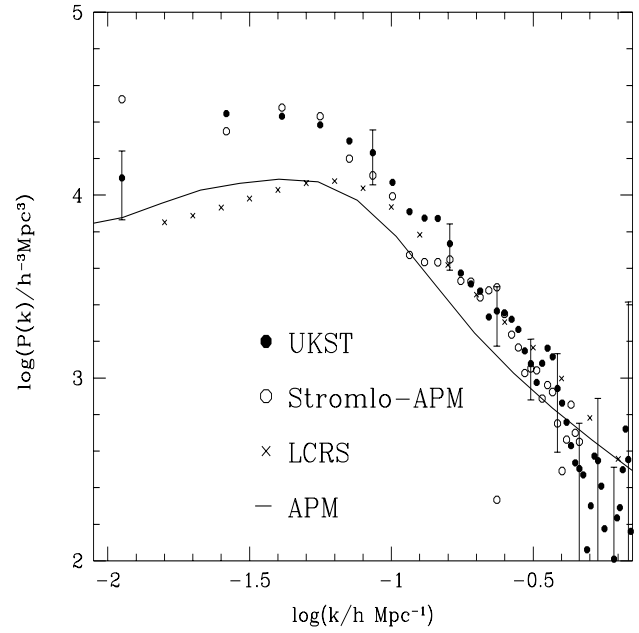


Figure 11. The flux limited, $P = 8000h^{-3}\text{Mpc}^3$, power spectrum of the Durham/UKST Survey (solid points) compared with the flux limited power spectra of other optical samples. The open circles show the power spectrum of the Stromlo-APM Survey (Tadros & Efstathiou 1996), again flux limited with $P = 8000h^{-3}\text{Mpc}^3$ and the crosses show the deconvolved $P(k)$ from the Las Campanas Redshift Survey from Lin et al (1996).

(Tadros & Efstathiou 1996) with the same selection (open circles). The two estimates of the power spectrum are in remarkably good agreement, except near wavenumbers of $\log k = -0.8, -0.5$ and -0.3 , where there are sharp dips in the Stromlo-APM power spectrum. The solid line shows the real space power spectrum measured from the APM Survey (Baugh & Efstathiou 1993), which is below the power spectra measured from the redshift surveys. We compare estimates of the power spectrum made from flux limited samples in Figure 11. Again, the filled circles show the power spectrum of the Durham/UKST Survey, the open circles show the Stromlo-APM Survey and the crosses show the power spectrum measured from the Las Campanas Survey (Lin et al 1996). The Durham/UKST and Stromlo-APM Surveys have similar magnitude limits, $b_J \sim 17$, whereas the Las Campanas Survey is approximately 1–1.5 magnitudes deeper, going to an R -band magnitude of $17.3 - 17.7$, depending upon the spectrograph used to measure redshifts in a particular field. The Las Campanas survey consists of six $1.5^\circ \times 80^\circ$ strips and an attempt has been made to deconvolve the survey window function from the estimate of the power spectrum plotted here (Lin et al 1996). The power spectra from flux limited samples are in good agreement down to a wavenumber of $\log k = -1.1$ or for scales $\lambda < 80h^{-1}\text{Mpc}$. On larger scales than this, the power spectrum measured from the Las Campanas Survey is below that obtained from the Durham/UKST and Stromlo-APM Surveys, which continue to rise to $\lambda \approx 150h^{-1}\text{Mpc}$. On scales larger than this, the convolution with the survey window function of these surveys affects the shape of the recovered power spectrum. Note that the weighting scheme used to

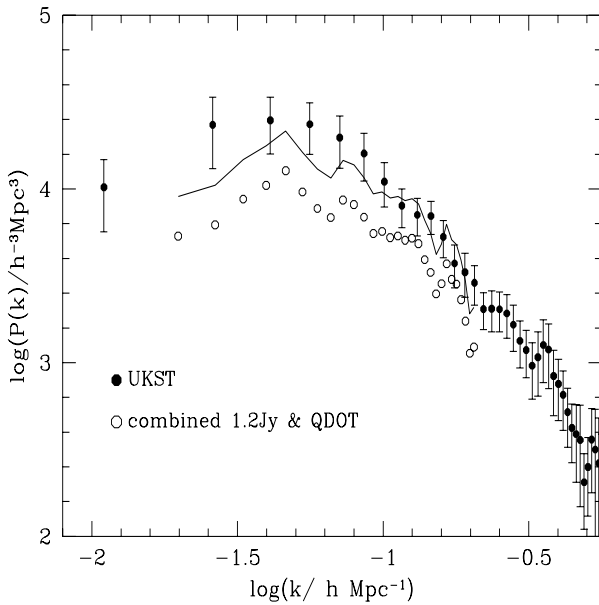


Figure 12. The power spectrum of Durham/UKST galaxies (filled circles) compared with the power spectrum (open circles) of IRAS galaxies obtained from the combined 1.2Jy and QDOT Surveys by Tadros & Efstathiou (1995). Both power spectra are measured from flux limited samples and are minimum variance estimates for the respective surveys. The line shows the IRAS power spectrum after multiplying by a relative bias factor squared of $b_{\text{IRAS}} = 1.3$, where we have assumed that the bias factor is not a function of scale.

estimate the Las Campanas power spectrum is different to that employed in this paper, with each galaxy weighted by the inverse of the selection function.

In Figure 12, we compare the power spectrum of the Durham/UKST Survey, which is an optically selected sample, with the power spectrum obtained from an analysis by Tadros & Efstathiou (1995) of the combined 1.2Jy Survey (Fisher et al 1995) and QDOT Survey (Efstathiou et al 1990) datasets, which are selected in the infra-red from the IRAS point source catalogue. We have plotted the minimum variance estimate of the power spectrum obtained for each dataset. The filled circles show the Durham/UKST power spectrum and the open circles show the power spectrum of IRAS galaxies. The IRAS galaxy power spectrum has a lower amplitude than the Durham/UKST power spectrum. The solid line shows the result of multiplying the IRAS power spectrum points by a constant, relative bias factor squared of $b_{\text{IRAS}} = 1.3$, which agrees with the value inferred by Peacock & Dodds (1994).

7 IMPLICATIONS FOR MODELS OF LARGE SCALE STRUCTURE

In this Section we compare the predictions of various scenarios for the formation of large scale structure in the universe with the power spectrum of the Durham/UKST Survey.

There are several steps that one has to go through in order to compare a power spectrum for the mass distribution, calculated in linear perturbation theory, with a galaxy

power spectrum measured using the positions of the galaxies inferred from their redshifts:-

- (i) Compute the nonlinear power spectrum of the mass distribution given the amplitude of *rms* density fluctuations specified by the value of σ_8 . We use the transformation given by Peacock & Dodds (1996).
- (ii) Choose a bias parameter, b , relating fluctuations in the mass distribution to fluctuations in the galaxy distribution: $P_{\text{gal}}(k) = b^2 P_{\text{mass}}(k)$. In the following analysis we make the simplifying assumption that the bias parameter is independent of scale.
- (iii) Model the distortion of clustering due to the fact that galaxy redshifts have a contribution from motions introduced by inhomogeneities in the local gravitational field of the galaxy as well as from the Hubble flow.
- (iv) Convolve the power spectrum with the window function of the Durham/UKST survey.

On large scales, (iii) leads to a boost in the amplitude of the power spectrum (Kaiser 1987), whilst on small scales the power is damped by random motions inside virialised groups and clusters. It is important to model these two extremes and the transition between them accurately, as this can have a significant effect on the shape of the power spectrum over the range of scales that we consider. We model the effects of the peculiar motions of galaxies on the measured power spectrum using the formula given by Peacock & Dodds (1994):

$$P_s(k) = b^2 P_r(k) G(\beta, y) \quad (8)$$

where $P_s(k)$ is the galaxy power spectrum measured in redshift space and $P_r(k)$ is the mass power spectrum measured in real space. The function $G(\beta, y)$, where $\beta = \Omega^{0.6}/b$ and $y = k\sigma/100$ (σ is the one dimensional velocity dispersion), is given by:-

$$\begin{aligned} G(\beta, y) = & \frac{\sqrt{\pi}}{8} \frac{\text{erf}(y)}{y^5} (3\beta^2 + 4\beta y^2 + 4y^4) \\ & - \frac{\exp[-y^2]}{4y^4} (\beta^2(3 + 2y^2) + 4\beta y^2). \end{aligned} \quad (9)$$

This assumes that the small scale peculiar velocities of galaxies are independent of separation and have a Gaussian distribution.

We compare the models with the Durham/UKST power spectrum measured from a sample with a volume limit defined by $z_{\text{max}} = 0.06$. This power spectrum measurement has larger errors than the minimum variance power spectrum from the flux limited sample on large scales, $\lambda = 2\pi/k \sim 60h^{-1}\text{Mpc}$. However, on scales smaller than this, the volume limited power spectrum has the smallest errors. Furthermore, the fractional errors in the power are smallest at high wavenumbers, because these waves are better sampled by the survey, and so it is these scales that are the most important for constraining the parameters in our model.

We test our simple model for the transformation of a linear theory power spectrum for mass fluctuations to a galaxy power spectrum measured in redshift space in Figure 13. The open circles show the mean power spectrum from 10 Durham/UKST mock catalogues, using the real space coordinates of the particles to map out the density. The filled circles show the distortion caused to the power spectrum when the peculiar motions of the particles are included. The

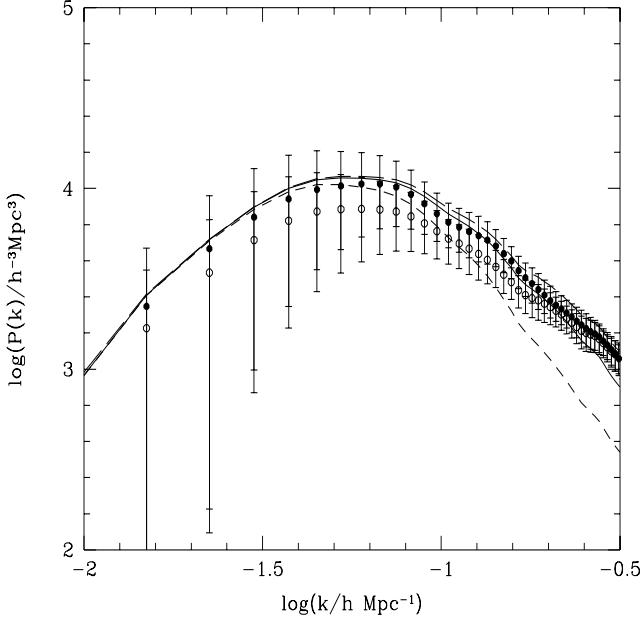


Figure 13. The power spectra of subsamples of particles drawn from the Hubble Volume simulation that are biased tracers of the mass distribution. The open circles show the mean power averaged over 10 mock Durham/UKST Surveys, with the density field calculated from the real space positions of the particles. The filled circles show the mean power in these mock catalogues when the redshift space coordinates of the particles are used to compute the density field. In both cases, the errorbars show the 1σ variance over the 10 mock catalogues. The lines show the results of applying the simple model for the transformation from a linear theory mass power spectrum to a galaxy power spectrum measured in redshift space, given by equation 8. We use a bias of $b = 1.5$ and vary the one dimensional velocity dispersion σ ; the long dashed line shows $\sigma = 300 \text{ km s}^{-1}$, the solid line shows $\sigma = 500 \text{ km s}^{-1}$ and the short dashed line shows $\sigma = 1000 \text{ km s}^{-1}$.

lines show the results of applying equation 8 to the linear theory τ CDM power spectrum. This equation results from performing an azimuthal average over the angle between the line of sight and the wavevector of the density fluctuation. The observer is also assumed to be at an infinite distance away from the wave. These two assumptions will mainly affect the longest wavelength fluctuations in a real survey that does not cover the whole sky. These scales are already distorted by the convolution with the survey window function. The model provides a reasonably good fit for a one dimensional velocity dispersion of $\sigma = 500 \text{ km s}^{-1}$, which is approximately the value found in the simulation (Jenkins et al 1998).

The first test we perform is to compare the power spectrum of APM Survey galaxies (Baugh & Efstathiou 1993, 1994a; Gaztañaga & Baugh 1998) with the Durham/UKST volume limited power spectrum. The APM power spectrum is measured in real space and is estimated by inverting the angular correlation function of APM galaxies with $17 \leq b_J \leq 20$. The shapes of the real space and redshift space power spectra can be compared in Figure 14(a). The real space power spectrum is shown by the dashed line, after multiplying by a constant factor of 1.4 to match the Durham/UKST Survey at small wavenumbers,

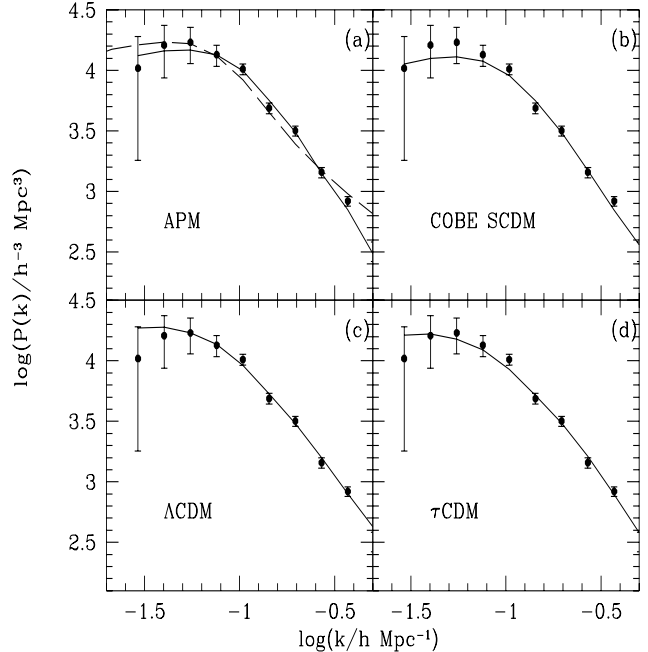


Figure 14. The points in each panel show the Durham/UKST power spectrum for a volume limited sample with $z_{\text{max}} = 0.06$. The power spectrum estimates have been rebinned to reduce the covariance in the errors. In (a), the dashed line shows the APM galaxy power spectrum measured in real space, rescaled to match the Durham/UKST power spectrum at large scales. The solid line shows the APM power spectrum, including the effects of distortion in redshift space. The remaining panels, b, c, d, show the best fitting curves for several variants of the Cold Dark Matter model. Table 1. gives the values of the linear bias b and the one dimensional velocity dispersion σ used in equation 9.

so that the relative shapes of the real space and redshift space power spectra can be readily compared. We have rebinned the Durham/UKST power spectrum and error bars to match the binning of the APM power spectrum which has $\delta \log k = 0.13$. The rebinned Durham/UKST power spectrum is shown in each panel of Figure 14 by the points and errorbars. The rebinning is done to reduce the covariance between the errors at different wavenumbers; the spacing of the power spectrum measurements is now much larger than the half width of the survey window function. We retain this binning of the Durham/UKST power spectrum in the subsequent analysis of theoretical power spectra below. As we are comparing two galaxy power spectra, we omit the factor of b^2 in equation 8. The best fitting APM galaxy power spectrum, including the redshift space distortions, is shown by the solid line in Figure 14(a). The transformation into redshift space removes the inflection in the real space APM power spectrum around a wavenumber of $k \sim 0.15 \text{ hMpc}^{-1}$. The best fitting values of β and σ , with 1σ errors are $\beta = 0.60 \pm 0.35$ and $\sigma = 320 \pm 140 \text{ km s}^{-1}$. Tadros & Efstathiou (1996) found $\beta = 0.38 \pm 0.67$ by comparing the Stromlo-APM redshift space power spectrum to the APM Survey power spectrum, restricting their attention to wavenumbers in the range $0.05 < k < 0.1 \text{ hMpc}^{-1}$, on which they argued that the damping of power in redshift space is negligible. The one dimensional velocity dispersion

Model	Ω_0	b	β	$\sigma \text{ km s}^{-1}$
ΛCDM	0.3	1.04 ± 0.09	0.47	520 ± 100
τCDM	1.0	1.64 ± 0.17	0.61	320 ± 110
SCDM	1.0	2.97 ± 0.26	0.34	1240 ± 200
COBE-SCDM	1.0	0.91 ± 0.1	1.10	760 ± 130

Table 1. The best fitting values of the bias parameter, b , and the one dimensional velocity dispersion, σ , for various different cosmological models. The errors are the 1σ errors obtained using the errorbars of the Durham/UKST power spectrum. We also give the value of β implied by our best estimate of the bias parameter b , for the density parameter Ω_0 of the model.

that we recover from the comparison is in excellent agreement with the measurement of Ratcliffe et al (1998c), but has much larger errors. By considering the galaxy correlation function binned in separation parallel and perpendicular to the line of sight, Ratcliffe et al obtained a value for the pairwise *rms* velocity dispersion along the line of sight of $\sigma_{||} = 416 \pm 36 \text{ km s}^{-1}$. This quantity is approximately $\sqrt{2}$ times the one dimensional velocity dispersion that we use, giving $\sigma = 294 \pm 25 \text{ km s}^{-1}$. If we add in quadrature the estimated error in the measured redshifts $\sim 150 \text{ km s}^{-1}$ (Ratcliffe et al 1998d), the Ratcliffe et al measurement implies $\sigma = 330 \text{ km s}^{-1}$.

We also test four popular Cold Dark Matter (CDM) models by treating the bias parameter and the one dimensional velocity dispersion as free parameters. The mass power spectra use the transfer function given in Efstathiou, Bond & White (1992). The models that we consider are; $\Omega_0 = 1$ CDM with a shape parameter $\Gamma = 0.5$ and with a normalisation of $\sigma_8 = 0.52$ (SCDM) that reproduces the local abundance of rich clusters (Eke, Cole & Frenk 1996); a model with a normalisation of $\sigma_8 = 1.24$ and $\Gamma = 0.5$ (COBE-SCDM), which matches the COBE detection of temperature anisotropies in the microwave background, but seriously over-predicts the abundance of hot clusters; τCDM , with $\Omega_0 = 1$, $\Gamma = 0.2$ and $\sigma_8 = 0.52$, which simultaneously matches the amplitude implied by COBE and by the cluster abundance through an adjustment to the shape of the power spectrum, as described in Section 3.4, and ΛCDM , which is a low density model, with a present day value for the density parameter of $\Omega_0 = 0.3$ and a cosmological constant of $\Lambda_0 = 0.7$ (Efstathiou, Sutherland & Maddox 1990). The ΛCDM model has a normalisation of $\sigma_8 = 0.93$.

The best fitting parameters are given in Table 1. Note that as we specify a value for the density parameter Ω_0 through our choice of structure formation model, we are constraining the value of the bias parameter b ; the implied errors on β are much smaller than if we had not selected a value for Ω_0 beforehand. For all the models considered, reasonable agreement with the Durham/UKST Survey power spectrum can be obtained if no restrictions are placed on the values of the bias and one dimensional velocity dispersion that are used in the fit. However, the SCDM and COBE-CDM models only produce a reasonable fit to the Durham/UKST power spectrum if large values of the velocity dispersion are adopted; these values are inconsistent with the value we obtain from the comparison with the APM Survey power spectrum at more than 3σ . The velocity dis-

persions required for the ΛCDM model is marginally inconsistent (1.5σ) with the value that we infer from the comparison with the APM power spectrum. This agrees with the results of the complementary analysis of the two point correlation function carried out by Ratcliffe et al (1998b), who analysed the clustering in a N-body simulation with a very similar cosmology and power spectrum. The τCDM model gives the best fit to the Durham/UKST data in the sense that the values of β and σ required are in excellent agreement with those obtained from the comparison with the real space galaxy power spectrum.

8 CONCLUSIONS

There is remarkably good agreement between measurements of the power spectrum of galaxy clustering made from optically selected surveys, on scales up to $\lambda = 60h^{-1} \text{ Mpc}$. On larger scales than this, only the most recently completed surveys cover a large enough volume to permit useful estimates of the power spectrum to be made. For scales larger than $\lambda = 60h^{-1} \text{ Mpc}$, we find good agreement between the power spectra of the Durham/UKST Survey and of the Stromlo-APM Survey (Tadros & Efstathiou 1996). We measure more power on these scales than is found in a clustering analysis of the Las Campanas Redshift Survey (Lin et al 1996). We find no convincing evidence for a dependence of galaxy clustering on intrinsic luminosity within the Durham/UKST Survey. However, we do measure a higher amplitude for the power spectrum from our optically selected sample compared with that recovered for galaxies selected by emission in the infrared; the offset in amplitude can be described by an optical/infrared bias factor of $b_{IRAS} = 1.3$.

We have compared the shape and amplitude of the APM Survey power spectrum (Baugh & Efstathiou 1993, 1994; Gaztañaga & Baugh 1998), which is free from any distortions caused by peculiar velocities, with the Durham/UKST power spectrum. The APM power spectrum displays an inflection at $k \sim 0.15h\text{Mpc}^{-1}$. Using a simple model for the effects of galaxy peculiar velocities that is valid over a wide range of scales, we find that the inflection is straightened out in redshift space. The APM power spectrum can be distorted to give a good match to the Durham/UKST power spectrum for $\beta = \Omega^{0.6}/b = 0.60 \pm 0.35$ and a one dimensional velocity dispersion of $\sigma = 340 \pm 120 \text{ km s}^{-1}$. These values are consistent with those found from an independent analysis of clustering in the Durham/UKST Survey by Ratcliffe et al (1998c), who obtained $\beta = 0.52 \pm 0.39$ (see Hamilton 1998 and references therein for estimates of β made from different surveys using a range of techniques) and $v_{12}(\sim \sqrt{2}\sigma) = 416 \pm 36 \text{ km s}^{-1}$. The value of β that we obtain from this analysis, can be used, with an assumption for the value of Ω_0 , to infer the amplitude of fluctuations in the underlying mass distribution. For example, if we assume $\Omega_0 = 1$, our value for β suggests that APM galaxies are biased with respect to fluctuations in the mass by $b = 1.7 \pm 1.0$; this in turn implies a value for the *rms* fluctuations in mass of $\sigma_8 = 0.84/b = 0.50 \pm 0.29$, which is consistent with that required to reproduce the abundance of massive clusters (Eke, Cole & Frenk 1996). As the abundance of clusters and β have a similar dependence on Ω_0 , this agreement will hold for any value of Ω_0 and therefore does not constrain Ω_0 .

We have compared theoretical models for structure formation with the power spectrum of the Durham/UKST survey. The best agreement is found with a variant of the Cold Dark Matter model known as τ CDM. A low density model with a cosmological constant also provides reasonable agreement, but for a velocity dispersion that is marginally inconsistent with that obtained from our comparison between the power spectra of the Durham/UKST and APM Surveys. Critical density CDM models with shape parameter $\Gamma = 0.5$ require one dimensional velocity dispersions that are much too high in order to provide a good fit to the Durham/UKST power spectrum. One possible way to resolve this problem would be to relax the assumption that the bias parameter between galaxies and the mass distribution is independent of scale. Whilst a constant bias is undoubtedly a poor approximation on scales around a few megaparsecs and smaller (see for example Benson et al 1998), our analysis probes scales greater than $20h^{-1}$ Mpc. A scale dependent bias on such large scales could be motivated in a cooperative galaxy formation picture (Bower, Coles, Frenk & White 1993), though the higher order moments of the galaxy distribution expected in such a model are not favoured by current measurements (Frieman & Gaztañaga 1994).

ACKNOWLEDGMENTS

FH acknowledges the receipt of a PPARC studentship. We would like to thank Helen Tadros for many helpful conversations and communicating data in electronic form for the Stromlo-APM Survey, Huan Lin for supplying LCRS $P(k)$ data, Shaun Cole for advice and a careful reading of the manuscript and Steve Hatton for assistance with the error analysis. Adrian Jenkins made the Hubble Volume simulation available to us, on behalf of the Virgo Consortium, and kindly provided us with essential software for reading the simulation output. We acknowledge the efforts of Alison Broadbent, Anthony Oates, Quentin Parker, Fred Watson, Richard Fong and Chris Collins in the construction of the Durham/UKST Survey. CMB acknowledges receipt of a computer equipment grant from the University of Durham.

REFERENCES

Baugh, C. M., & Efstathiou, G., 1993, MNRAS, 265, 145
 Baugh, C. M., & Efstathiou, G., 1994a, MNRAS, 267, 323
 Baugh, C. M., & Efstathiou, G., 1994b, MNRAS, 270, 183
 Benson, A. J., Cole, S., Frenk, C. S., Baugh, C. M. & Lacey, C. G., 1999, MNRAS, submitted.
 Bower, R. G., Coles, P., Frenk, C. S., & White, S. D. M., 1993, ApJ, 405, 403
 Cole, S. M., Hatton, S. J., Weinberg, D. H. & Frenk, C. S., 1998, MNRAS, 300, 945
 Collins, C. A., Heydon-Dumbleton, N. H. & MacGillivray, H. T., 1988, MNRAS, 236, 7p
 Collins, C. A., Nichol, R. C., Lumsden, S. L., 1992, MNRAS, 254, 295
 Davis, M., Efstathiou, G., Frenk, C. S., White, S. D. M., 1985, ApJ, 292, 371
 Efstathiou, G., Kaiser, N., Saunders, W., Lawrence, A., Rowan-Robinson, M., Ellis, R.S., Frenk, C.S., 1990, MNRAS, 247, 10p
 Efstathiou, G., Bond, J.R., White, S.D.M., 1992, MNRAS, 258, 1
 Efstathiou, G., Sutherland, W. J., Maddox, S. J., 1990, Nature, 348, 705
 Eke, V.R., Cole, S., Frenk, C.S., 1996, MNRAS, 282, 263
 Feldman H. A., Kaiser N., Peacock J. A., 1994, ApJ, 426, 23
 Fisher, K.B., Huchra, J.P., Strauss, M.A., Davis, M., Yahil, A., Schlegel, D., 1995, ApJS, 100, 69
 Frieman, J. A., & Gaztañaga, E., 1994, ApJ, 425, 392
 Gaztañaga, E., Baugh, C.M., 1998, MNRAS, 294, 229
 Hamilton, A. J. S., 1993, ApJ, 417, 19
 Hamilton, A. J. S., 1998, in 'The Evolving Universe', ed D. Hamilton, p185, Kluwer Academic (astro-ph/9708102).
 Jenkins, A., et al 1998, ApJ, 499, 20
 Kaiser, N., 1987, MNRAS, 227, 1
 Landy, S. D., & Szalay, A. S., 1993, ApJ, 412, 64
 Lin, H., Kirshner, P., Shectman S.A., Landy, S. D., Oemler, A., Tucker, D. L. & Schechter, P. L., 1996, ApJ, 471, 617
 Loveday, J., Maddox, S.J., Efstathiou, G., Peterson, B.A., 1995, ApJ, 442, 457
 Maddox, S.J., Efstathiou, G., Sutherland, W. J., 1996, MNRAS, 283, 1227
 Maddox, S. J., Sutherland, W. J., Efstathiou, G. P., Loveday, J., 1990, MNRAS, 242, 43P
 Park, C., Vogeley, M. S., Geller, M. J., Huchra, J. P., 1994, APJ, 431, 569
 Parker, Q.A., & Watson, F. G., 1995 in Maddox, S.J., Aragón-Salamanca, A., eds., 35th Herstmonceux Conf. Cambridge, Wide Field Spectroscopy and the Distant Universe, Princeton Univ. Press, Princeton, NJ, p33
 Peacock, J. A., & Nicholson, D., 1991, MNRAS, 253, 307
 Peacock, J. A., & Dodds, S. J., 1994, MNRAS, 267, 1020
 Peacock, J. A., & Dodds, S. J., 1996, MNRAS, 280, L19
 Ratcliffe, A. 1996, PhD Thesis, University of Durham
 Ratcliffe, A., Shanks, T., Parker, Q. A., Fong, R., 1996, MNRAS 281, L47
 Ratcliffe, A., Shanks, T., Parker, Q. A., Fong, R., 1998a, MNRAS, 293, 197
 Ratcliffe, A., Shanks, T., Parker, Q. A., Fong, R., 1998b, MNRAS, 296, 173
 Ratcliffe, A., Shanks, T., Parker, Q. A., Fong, R., 1998c, MNRAS, 296, 191
 Ratcliffe, A., Shanks, T., Parker, Q. A., Broadbent, A., Watson, F.G., Collins, C.A., Fong, R., 1998d, MNRAS, 300, 417
 Rowan-Robinson, M., Saunders, W., Lawrence, A., Leech, K. 1991, MNRAS, 253, 485
 Shectman, S.A., Landy, S.D., Oemler, A., Tucker, D.L., Lin, H., Kirshner, R.P., Schechter, P.L., 1996, ApJ, 470, 172 Tadros, H., & Efstathiou,G., 1995, MNRAS, 276, L45
 Tadros, H., & Efstathiou,G., 1996, MNRAS, 282, 1381
 Tegmark, M., Hamilton, A., Strauss, M., Vogeley, M., Szalay, A., 1998, ApJ, 499, 555
 White, S.D. M., Efstathiou, G., Frenk, C.S., 1993, MNRAS, 262, 1023
 White, M., Gelmini, G., Silk, J., 1995, Physical Review D, 51, 2669

APPENDIX:

$kh\text{Mpc}^{-1}$	$P(k)_{vol,z_{\max}=0.06}$	1σ	$P(k)_{flux,P=4000}$	1σ	$P(k)_{flux,P=8000}$	1σ
0.026	8178.6	8287.9	23373.5	10300.0	27910.5	11560.5
0.041	16153.0	12867.0	24827.5	8945.7	26962.0	9936.2
0.056	17014.0	10170.0	23595.5	7804.6	24177.0	8555.5
0.071	13927.0	6466.5	19763.0	6602.0	19774.5	7242.8
0.056	17014.0	10170.0	23595.5	7804.6	24177.0	8555.5
0.071	13927.0	6466.5	19763.0	6602.0	19774.5	7242.8
0.086	12215.0	4671.6	15992.0	4880.0	17048.5	5684.4
0.101	11018.0	3450.4	11005.0	3148.6	11743.0	3459.8
0.116	8710.3	2370.3	8001.1	2014.6	8120.3	2356.0
0.131	6141.0	1721.2	7094.5	1723.7	7486.9	2085.1
0.146	4478.2	1144.1	6981.9	1505.9	7462.8	2006.1
0.161	4021.4	849.1	5296.6	1271.9	5424.6	1533.4
0.176	3859.1	803.5	3728.6	1036.8	3744.8	1184.7
0.191	3490.1	788.9	3319.8	938.7	3261.4	1096.8
0.206	2941.9	604.5	2879.6	737.1	2989.8	962.5
0.221	2397.8	447.9	2034.8	486.0	2155.2	654.3
0.236	1930.3	368.9	2044.2	541.4	2321.9	831.9
0.251	1705.7	372.6	2029.2	523.5	2268.6	746.2
0.266	1494.9	335.3	1922.2	542.4	2093.0	719.5
0.280	1282.2	250.5	1654.8	493.8	1839.7	665.3
0.295	1150.0	186.6	1335.8	403.0	1405.9	512.5
0.310	1068.9	183.4	1179.8	359.1	1194.9	434.8
0.325	960.3	187.4	960.0	343.1	944.6	404.5
0.340	871.3	197.5	1075.0	432.6	1203.0	620.5
0.355	907.0	223.9	1264.6	498.2	1456.3	830.1
0.370	893.8	216.8	1190.2	481.1	1306.3	742.9
0.385	816.7	207.6	838.3	342.5	875.4	481.9
0.400	769.8	213.0	755.1	290.8	729.3	382.5
0.415	741.3	211.0	652.8	245.0	573.0	302.7
0.430	701.5	215.1	519.0	194.1	426.3	215.3
0.445	615.4	213.0	421.4	155.9	343.6	198.6
0.460	478.7	171.9	388.1	182.7	318.9	245.9
0.475	365.1	128.8	358.5	210.5	295.1	300.7
0.490	256.2	98.4	204.9	95.0	115.0	96.0
0.505	195.7	83.4	250.6	119.5	199.8	153.4
0.520	177.4	88.1	361.3	183.5	373.9	311.7
0.535	245.2	133.6	316.3	222.9	353.5	419.1
0.550	307.3	190.7	263.7	217.3	256.1	364.7
0.565	304.1	201.6	210.3	178.4	149.8	236.1
0.580	291.0	195.7	66.8	66.4	66.0	133.2
0.595	336.5	250.2	89.9	98.5	5.9	15.1
0.610	343.9	255.4	150.2	145.1	102.2	222.8
0.625	303.4	239.3	209.4	211.6	171.5	371.1
0.640	209.3	212.5	222.4	241.8	195.3	384.7
0.655	82.9	103.0	328.2	609.4	314.8	1097.8
0.669	54.1	64.0	462.6	1112.6	526.5	2583.1
0.684	221.1	234.4	324.5	709.5	357.2	2247.5
0.699	448.5	482.8	255.1	468.5	144.8	490.4

Table A1. Measurements of the power spectrum from the Durham/UKST Survey. The first column gives the wavenumber. The power has been rebinned into $\delta k = 0.015h^{-1}\text{Mpc}^{-1}$ bins, roughly the width at half maximum of the power spectrum of the survey window function, to reduce the correlation between bins. The second column gives the power measured in a volume limited sample with $z_{\max} = 0.06$. The fourth and sixth columns give the power measured in the flux limited Durham/UKST Survey, when weights of $P = 4000h^{-3}\text{Mpc}^3$ and $P = 8000h^{-3}\text{Mpc}^3$, respectively are used in equation 1. Columns 3, 5 and 7 gives the 1σ errors on each measurement. The errors are the 1σ variance from 40 mock catalogues extracted from the Hubble Volume.